The application of Landsat-8 OLI/TIRS data for geological mapping: a case study from SE Iran

Amin Beiranvand Pour[1*], Mazlan Hashim[1]

[1]Institute of Geospatial Science & Technology (INSTeG) Universiti Teknologi Malaysia

81310 UTM Skudai, Johor Bahru, Malaysia

Email address: beiranvand.amin80@gmail.com; profmhashim@gmail.com

Abstract

New generations of advanced remote sensing data have been used by Earth scientists over last decades. This study presents the applicability of recently launched Landsat-8 data for geological mapping. It has two sensors, namely Operational Land Imager (OLI) and the Thermal Infrared Sensor (TIRS) collect image data in nine visible, near-infrared, shortwave infrared bands and two longwave thermal bands. Sar Cheshmeh copper mining district in the southeastern part of the Urumieh-Dokhtar volcanic belt, SE Iran has been selected as a case study to show the capability of Landsat-8 bands for hydrothermal alteration and lithological mapping. Image processing results indicate that structural features and textural characteristics of igneous and sedimentary rocks, vegetated part and iron oxide minerals can be easily identified by visible and near-infrared (2 to 5) bands. Hydrothermal alteration areas associated with known copper deposits are distinguishable using shortwave infrared bands (6 and 7). Silicate minerals and lithological boundary are detectable using thermal bands at regional scale. Thermal infrared bands of Landsat-8 significantly improved the quality and availability of thermal infrared remote sensing data for geological mapping, which is broadly applicable for geological purposes in the future.

Key words: Landsat-8 data, Operational Land Imager, Thermal Infrared Sensor, Geological mapping.

1. Introduction

The Landsat satellites era that began in 1972 will become a nearly 42-year global land record with the successful launch and operation of the Landsat Data Continuity Mission (LDCM). Two generations of Landsat satellites has been launched by National Aeronautics and Space Administration (NASA) and the U.S. Geological Survey (USGS).The first generation (Landsats 1, 2, and 3) operated from 1972 to 1985 and is essentially replaced by the second generation (Landsats 4, 5, and 7), which began in 1982 and continues to the present. Landsat 6 of the second generation was launched in 1993, but failed to reach orbit (Sabins, 1999). The LDCM is a partnership formed between the NASA and the USGS to place the next Landsat satellite in orbit.

Landsat-8 was launched on 4 February 2013 from Vandenberg Air Force Base in California. It is an American Earth observation satellite and the eighth satellite in the Landsat program. Landsat-8 joins Landsat-7 on-orbit, providing increased coverage of the Earth's surface. It is in the form of free-flyer spacecraft carrying a two-sensor payload, the Operational Land Imager (OLI) and the Thermal Infrared Sensor (TIRS). These two instruments collect image data for nine visible, near-infrared, shortwave infrared bands and two longwave thermal bands. They have high signal to noise (SNR) radiometer performance, enabling 12-bit quantization of data allowing for more bits for better land-cover characterization. Landsat-8 provides moderate-resolution imagery, from 15 meters to 100 meters of Earth's surface and polar regions (Ariza, 2013). Landsat-8 data have been distributed to the general public on nondiscriminatory basis at no cost to the user. The data can be easily downloaded from the (http://earthexplorer.usgs.gov and http://glovis.usgs.gov/) online linkages.

This study evaluates the capability Landsat-8 data for mapping hydrothermal alteration area and lithological units. Sar Cheshmeh copper mining district has been selected as a case study, which is located in the southeastern part of the Urumieh-Dokhtar volcanic belt, SE Iran (Fig. 1), where Cu and Mo are actively being mined.

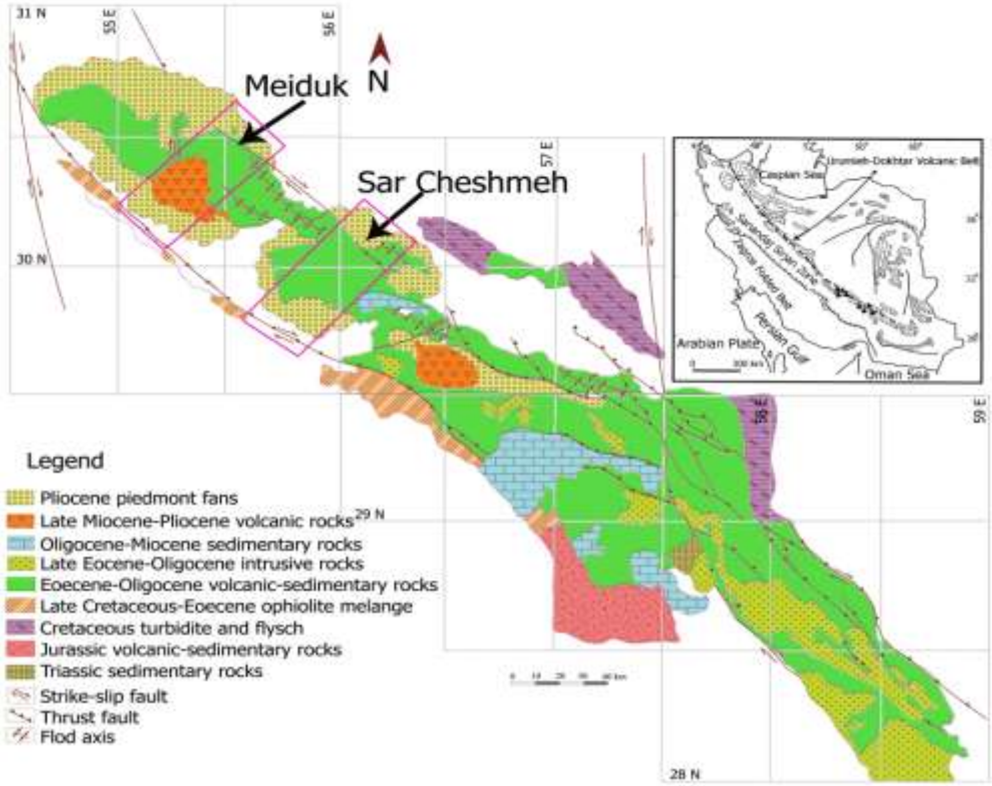

Fig.1. Simplified geology map of southeastern segment of the Urumieh–Dokhtar volcanic Belt (modified after Pour and Hashim, 2012b). Study areas are located in rectangles.

2. Material and methods

2.1 Landsat-8 OLI/ TIRS Data

A cloud-free level 1T (terrain corrected) Landsat-8 image LC81600392013135LGN01 (Path/Row 160/39) were obtained through the U.S. Geological Survey Earth Resources Observation and Science Center (EROS) (http://earthexplorer.usgs.gov). It was acquired on May 15, 2013 for the Sar Cheshmeh area. The image map projection is UTM zone 40 North (Polar Stereographic for Antractica) using the WGS-84 datum. The Operational Land Imager (OLI) feature two additional spectral channels with advanced measurement capabilities include: a deep-blue band for coastal water and aerosol studies (band 1, 0.433-0.453 µm, 30 m pixel size), and a band for cirrus cloud detection (band 9, 1.360-1.390 µm, 30 m pixel size). The Thermal Infrared Sensor (TIRS) collects data in two long wavelength thermal bands (band 10, 10.30-11.30 µm, 100 m pixel size; band 11, 11.50-12.50 µm, 100 m pixel size), which have already been co-registered with OLI data (Table 1). Landsat-8 image of target site was processed using the ENVI (Environment for Visualizing Images) version 4.8 software package.

2.2 Preprocessing of Landsat-8 OLI/ TIRS Data

Landsat-8 data were converted to surface reflectance using the Internal Average Relative Reflection (IARR) method (Ben-Dor et al., 1994). Ben-Dor et al. (1994) recommended IARR reflectance technique for mineralogical mapping as a preferred calibration technique, which does not require the prior knowledge of samples collected from the field. During the atmospheric correction, raw radiance data from imaging spectrometer is re-scaled to reflectance data. Therefore, all spectra are shifted to nearly the same albedo. The resultant spectra can be compared with the reflectance spectra of the laboratory or filed spectra, directly. The panchromatic and cirrus cloud (band 9) bands have not been used in this study.

2.3 Image processing methods

To evaluate the Landsat-8 data different Red-green-Blue (RGB) color combination images band ratios were applied for enhancing the hydrothermally altered rocks, lithological units at regional scale. Band ratioing is a technique where

the digital number value of one band is divided by the digital number value of another band. Band ratios are very useful for highlighting certain features or materials that cannot be seen in the raw bands (Inzana et al., 2003, Pour et al, 2013, 2014).
Spectral mapping methods aim at extracting individual mineral species from a mixed pixel spectrum, in theory providing geologist with the capability to map mineral surface composition. Although these image processing methods have been mostly applied on hyperspectral data, they can also be applicable logically to multispectral data. With these image processing methods, pixels that have mixed spectral signatures will be extractable and can be separated from the undesirable background. Thus, mineral abundance maps can be produced free of diluting effects of surrounding environment. Analytical imaging and geophysics (AIG)-developed hyperspectral analysis processing methods (Kruse and Boardman, 2000) are applied on Landsat-8 bands for mapping hydroxide and carbonate minerals assemblages in hydrothermal alteration zones. AIG approach for analysis of hyperspectral data are implemented and documented within the ENVI software system. Data are analyzed using AIG approach to determine unique spectral end-members and their spatial distribution, abundances and producing detailed mineral maps (Kruse et al., 2003).

3. Results and discussion

RGB color combination image was allocated to near infrared (band 5: 0.845-0.885 μm) and short wavelength infrared bands (band 6:1.560-1.660 μm , band 7: 2.100-2.300 μm) of Landsat-8 data, respectively. Figure 2 shows the resultant full scene image for the study area. Geological features, including textural characteristics of the igneous and sedimentary rocks, structural features and vegetation are clear. Vegetated areas are appeared as light red color in the scene.

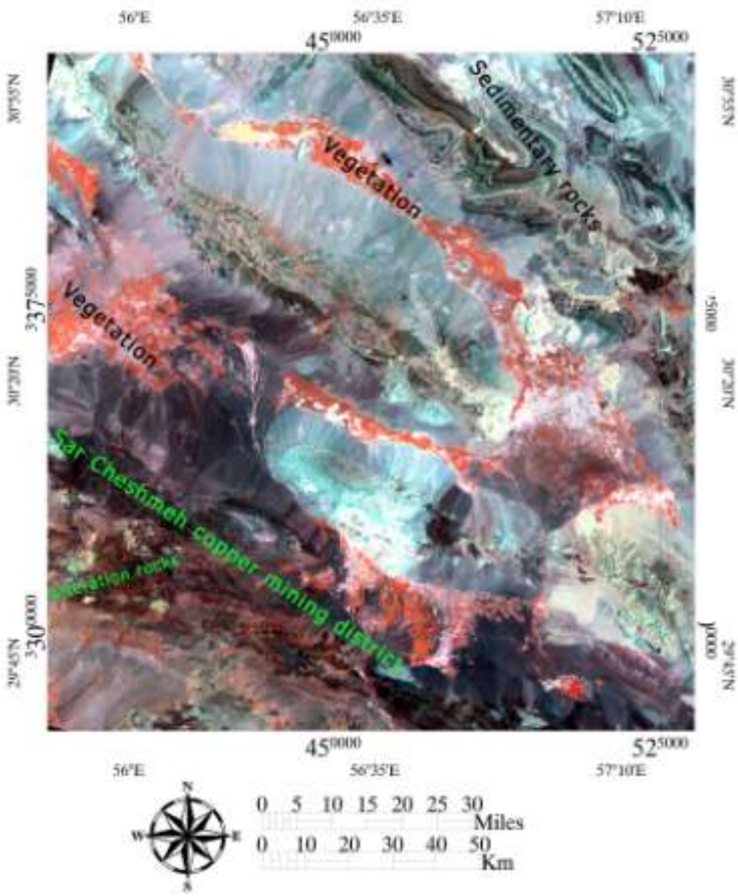

Fig. 2. RGB color combination image of band 5, 6 and 7of Landsat-8 data.

Figure 3 shows RGB color combination image of band 10 (10.30-11.30 μm), 11 (11.50-12.50 μm) and 7 (2.100-2.300 μm) of Landsat-8 at a regional scale. Rocks with high emissivity value attributed to high silicate minerals in their composition are manifested as red color in the image. On the other hand, rocks with moderate and low emissivity value are appeared as pink and blue colors, respectively (Fig. 3).

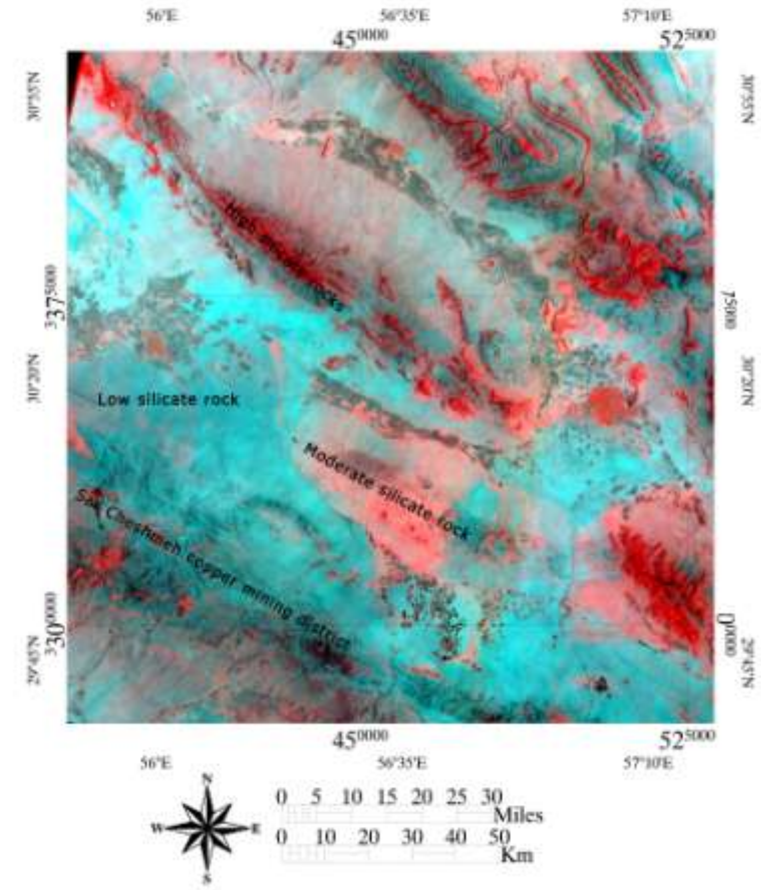

Fig. 3. RGB color combination image of band 10, 11 and 7 of Landsat-8 data.

AIG approach has been applied on 9 Landsat-8 bands. These bands linearly transformed using MNF methods. MNF component images show steadily decreasing image quality with increasing band number, so images with higher eigenvalues contain higher spectral information (Pour and Hashim, 2011, 213, 2012a,b; 2014 a,b). RGB color combination image was assigned to three high eigenvalues MNF transformed bands. Figure 4 shows the resultant image, lithological units and hydrothermally altered rocks are discriminated in the image. Elliptical and circular patterns of hydrothermally altered rocks are appeared as purple color around known copper deposits in the study area (Fig. 4). It should be noted that hydrothermally altered rocks associated with porphyry copper mineralization are located in crystalline igneous rocks background. The existence of thermal infrared spectral information in the MNF transformed images assist to identification of crystalline igneous rocks background, which is manifested as light blue color in the scene (Fig. 4).

The output of MTMF is a set of rule images given as MF and infeasibility scores for each pixel related to each end-member. Four end-members extracted from the image and identified based on comparing with known spectra from USGS spectral libraries, including vegetation, iron oxide minerals, clay and carbonate minerals and silicate minerals. Figure 5 shows MF score image of clay and carbonate minerals for the study area. Green areas are high digital number (DN) value pixels above the background with low infeasibility (Fig. 5). Most of the identified areas are associated with the known porphyry copper deposits and few of them can be seen in the sedimentary rock background (Northwestern part of the scene) in the study area.

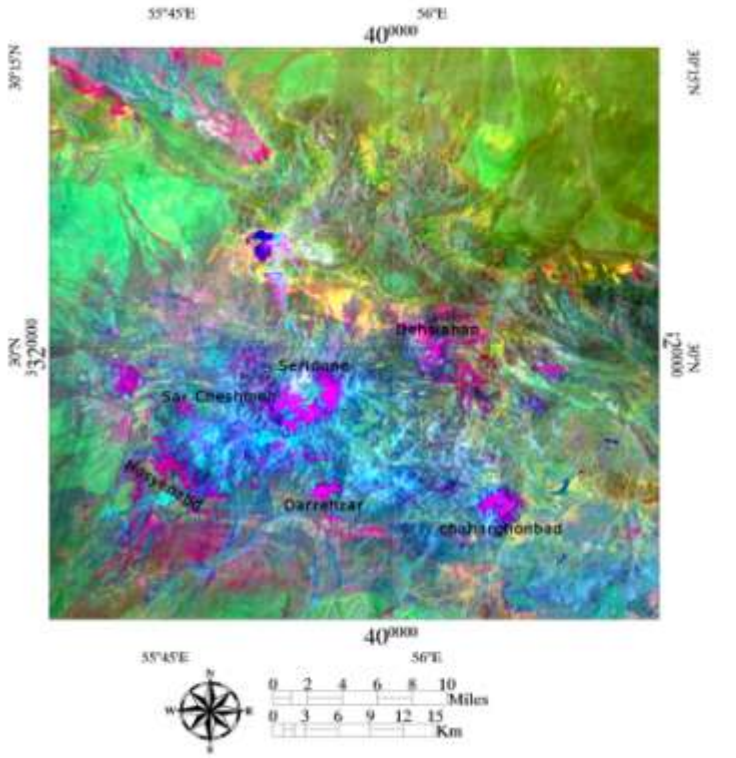

Fig.4. RGB color combination of MNF 1, 2, 3 components.

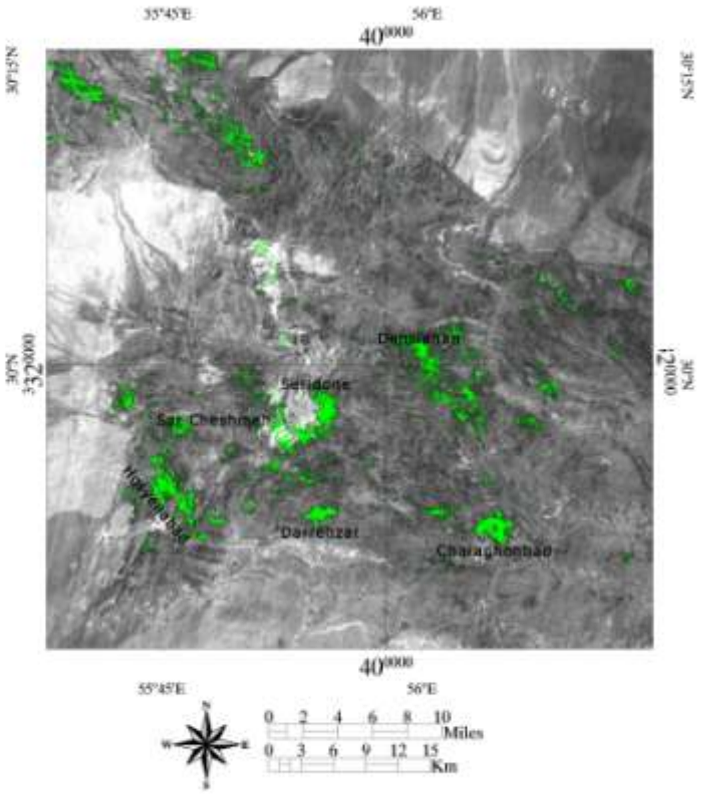

Fig.5. MF score image of clay and carbonate minerals.

4. Conclusions

This study evaluates the applicability of Landsat-8 data to extract geologic information for hydrothermal alteration and lithological mapping using some selected image processing methods. Sar Cheshmeh copper mining districts in southeastern segment of the Urumieh-Dokhtar Volcanic Belt, SE Iran has been selected as case study. Results indicate that Landsat-8 bands have great ability to yield spectral information for identifying vegetation, iron oxide/hydroxide and clay and carbonate minerals, silicate mineral and lithological units at both regional anddistrict scales. The TIR bands of Landsat-8 significantly improved the quality and availability of TIR remote sensing data for geological mapping. This investigation demonstrates significant implications for geologists to utilize Landsat-8 OLI/TIRS data for geological purposes in the future.

Acknowledgements
This study was conducted as a part of Fundamental Research Grant scheme (FRGS) (Vote no: R.J130000.7809.4F455) granted by *Universiti Teknologi Malaysia* (UTM).

References

Ariza. A., 2013. Landsat data continuity mission,version1.0. INSTITUTO GEOGRÁFICO AGUSTÍN CODAZZI Bogotá. Colombia 2013.

Ben-Dor, E., Kruse, F.A., Lefkoff, A.B. and Banin, A., 1994. Comparison of three calibration techniques for utilization of GER 63-channel aircraft scanner data of Makhtesh Ramon, Nega, Israel. Photogrammetric Engineering and Remote Sensing, 60(11), 1339-1354.

Inzana, J., Kusky, T., Higgs, G ., Tucker, R., 2003. Supervised classifications of Landsat TM band ratio images and Landsat TM band ratio image with radar for geological interpretations of central Madagascar. Journal of African Earth Sciences. 37, 59-72.

Kruse, F.A., Boardman, J.W., 2000. Characterization and Mapping of Kimberlites and Related Diatremes Using Hyperspectral Remote Sensing. IEEE Tran. Geos. Remote Sensing, 0-7803-5846-5.

Kruse, F.A., Bordman, J.W., Huntington, J.F., 2003. Comparison of airborne hyperspectral data and EO-1 Hyperion for mineral mapping. IEEE Trans.Geosc. Remote Sensing, 41(6), 1388-1400.

Pour, B.A. and Hashim, M., 2011. Identification of hydrothermal alteration minerals for exploring of porphyry copper deposit using ASTER data, SE Iran. Journal of Asian Earth Sciences, 42, 1309-1323.

Pour, B.A. and Hashim, M., 2012a. The application of ASTER remote sensing data to porphyry copper and epithermal gold deposits. Ore Geology Reviews. 44, 1-9.

Pour, B. A. and Hashim, M., 2012b. Identifying areas of high economic-potential copper mineralization using ASTER data in Urumieh-Dokhtar Volcanic Belt, Iran. Advances in Space Research 49, 753-769.

Pour, B.A. and Hashim, M., 2013. Fusing ASTER, ALI and Hyperion data for enhanced mineral mapping. International Journal of Image and Data Fusion. 4, 126-145.

Pour, B. A., Hashim, M, and van Genderen. J. 2013. Detection of hydrothermal alteration zones in a tropical region using satellite remote sensing data: Bau gold field, Sarawak, Malaysia. Ore Geology Reviews. 54, 181-196.

Pour, B. A., Hashim, M, Marghany. M., 2014. Exploration of gold mineralization in a tropical region using Earth Observing-1 (EO1) and JERS-1 SAR data: a case study from Bau gold field, Sarawak, Malaysia. Arabian Journal of Geosciences. 7, 2393-2406.

Pour, B. A., Hashim, M., 2014a. Alteration mineral mapping using ETM+ and hyperion remote sensing data at Bau Gold Field, Sarawak, Malaysia. IOP Conference Series: Earth and Environmental Science 18 (1), 012149.

Pour, B. A., Hashim, M., 2014b. Structural geology mapping using PALSAR data in the Bau gold mining district, Sarawak, Malaysia. Advances in Space Research, 54, 644-654.

Sabins, F.F., 1999. Remote sensing for mineral exploration. Ore Geology Reviwes,14, 157-183.